

Fatigue Life Calculation of Metastable Austenitic Steels

*M. Smaga¹, F. Walther², *D. Eifler¹

¹ *Institute of Materials Science and Engineering, University of Kaiserslautern,
Kaiserslautern, Germany;*

² *Schaeffler KG, Corporate Basic Projects and Long Term Quality,
Herzogenaurach, Germany*

Abstract

Monotonic and cyclic Plastic deformation of metastable austenitic steels can lead to a phase transformation from paramagnetic austenite to ferromagnetic α' -martensite. The deformation-induced changes of the magnetic properties are directly related to the accumulated plastic strain and therefore to the actual fatigue state. This paper includes a detailed characterization of the deformation-induced austenite-martensite-transformation in the metastable austenitic steels AISI 304, AISI 321 and AISI 348. The cyclic deformation behavior is evaluated by mechanical stress-strain hysteresis as well as high-precision temperature measurements. With in-situ ferritoscope magnetic measurements, the development of the α' -martensite and the change in the magnetic induction due to the Villari effect were investigated. On the basis of far-reaching cross effects of mechanical and magnetic properties, measurements of magnetic-mechanical hysteresis loops were performed. Hence, a method for fatigue life calculation based on the change in magnetic properties has been developed.

1. Introduction

Several austenitic steels are known to be metastable at ambient temperature. Plastic deformation of this steels often leads to a phase transformation from paramagnetic austenite (Fig. 1a) into ferromagnetic α' -martensite (Fig. 1b) [1-2]. As a consequence of this phase transformation a change of mechanical properties, e.g. TRIP-effect (Transformation-Induced Plasticity) and changes of magnetic properties [3-5] occur. An empirical relation between the α' -martensite fraction and the amount of plastic strain during isothermal monotonic loading was investigated in [6] and mathematically described in [7]. Only a few models exist for the deformation-induced α' -austenite-martensite transformation under cyclic loading [8-9].

*Corresponding Authors:

Prof. Dr.-Ing. habil. Dietmar Eifler

eifler@mv.uni-kl.de

Dr.-Ing. Marek Smaga

smaga@mv.uni-kl.de

Institute of Materials Science and Engineering

University of Kaiserslautern, Germany

P. O. Box: 30 49

D-67653 Kaiserslautern, Germany

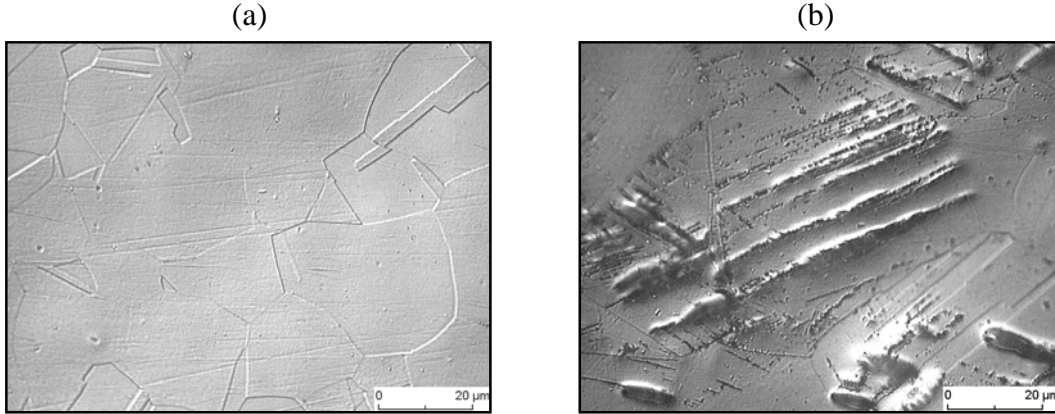


Fig. 1: Optical micrographs of austenite after solution annealing (a) and after plastic deformation with α' -martensitic needles in an austenitic matrix (b)

The change in the magnetic properties of materials are directly influenced by static and cyclic loading. Therefore actual research activities focus on using of the change in defined magnetic properties for the evaluation of fatigue processes and fatigue life calculation [10]. At present TRIP-steel sensors [11] are used to measure peak strains due to overloads at bridges. The formation of α' -martensite directly correlates with the actual fatigue state and can be measured with non-destructive magnetic methods. The mathematical description of the correlation between the α' -martensite fraction and fatigue life as well as the application of non-destructive magnetic testing methods to quantify the portion of α' -martensite are fundamental requirements for a reliable and cost-effective application of metastable austenitic steels.

2. Materials

The investigated materials are the low carbon chromium-nickel austenitic steels AISI 304 (X5CrNi1810, 1.4301), AISI 321 (X6CrNiTi1810, 1.4541) and AISI 348 (X10CrNiNb189, 1.4546). The chemical composition of (AISI 304) as well as additionally titanium- (AISI 321) and niobium-alloyed (AISI 348) austenites are given in Tab. 1. By the additional alloying with titanium or niobium the formation of chromium carbides, which can yield to chromium depletion at the grain boundaries, and therefore intergranular corrosion is reduced, since these elements form titanium and niobium carbides due to their high carbon affinity.

Material	C	Cr	Ni	Ti	Nb	Mn	Mo	N	Cu	Si
AISI 304	0.03	18.42	9.05	0.02	0.03	1.75	0.37	0.05	0.03	0.58
AISI 321	0.03	17.34	9.90	0.12	0.03	1.74	0.28	0.02	0.03	0.45
AISI 348	0.04	17.41	9.29	0.02	0.37	1.54	0.26	0.02	0.03	0.41

Table 1: Chemical composition in weight -%

$$M_S = 1350 - 1665 \cdot (C + N) - 42 \cdot Cr - 61 \cdot Ni - 28 \cdot Si - 33 \cdot Mn \text{ [}^\circ\text{C]} \quad (1)$$

$$M_{d30} = 413 - 462 \cdot (C + N) - 9.2 \cdot Si - 8.1 \cdot Mn - 13.7 \cdot Cr - 9.5 \cdot Ni - 18.5 \cdot Mo \text{ [}^\circ\text{C]} \quad (2)$$

A large number of technically relevant chromium-nickel steels exist at ambient temperature in the metastable state. Due to plastic deformation these metastable austenites can be transformed into α' -martensite. The chemical composition has a fundamental influence on the austenite stability, which can be described with the martensite start temperature M_S for thermally induced α' -martensite formation and with the so-called M_{d30} temperature for deformation-induced α' -martensite formation. At M_{d30} temperature by definition 50 % α' -martensite is formed as a result of 30 % plastic deformation. Empirical equations have been derived for M_S (Eq. 1) and M_{d30} (Eq. 2), respectively [12]. Decreasing M_S and M_{d30} temperatures are combined with an increasing austenite stability. Due to minimum M_S and M_{d30} temperatures AISI 304 is more stable compared to the titanium-alloyed AISI 321 and the niobium-alloyed AISI 348 steels (Tab. 2).

Material	$R_{p0.2}$ [MPa]	$R_{p1.0}$ [MPa]	R_m [MPa]	A_5 [%]	M_S [°C]	M_{d30} [°C]
AISI 304	248	286	606	39	-182	12
AISI 321	190	226	581	37	-129	37
AISI 348	270	308	640	33	-113	37

Table 2: Monotonic properties, M_S and M_{d30} temperatures

Due to a ratio of yield strength $R_{p0.2}$ to tensile strength R_m below 0.71 cyclic hardening is expected for these steels. AISI 348 is characterized by maximum and AISI 321 by minimum values (Tab. 2).

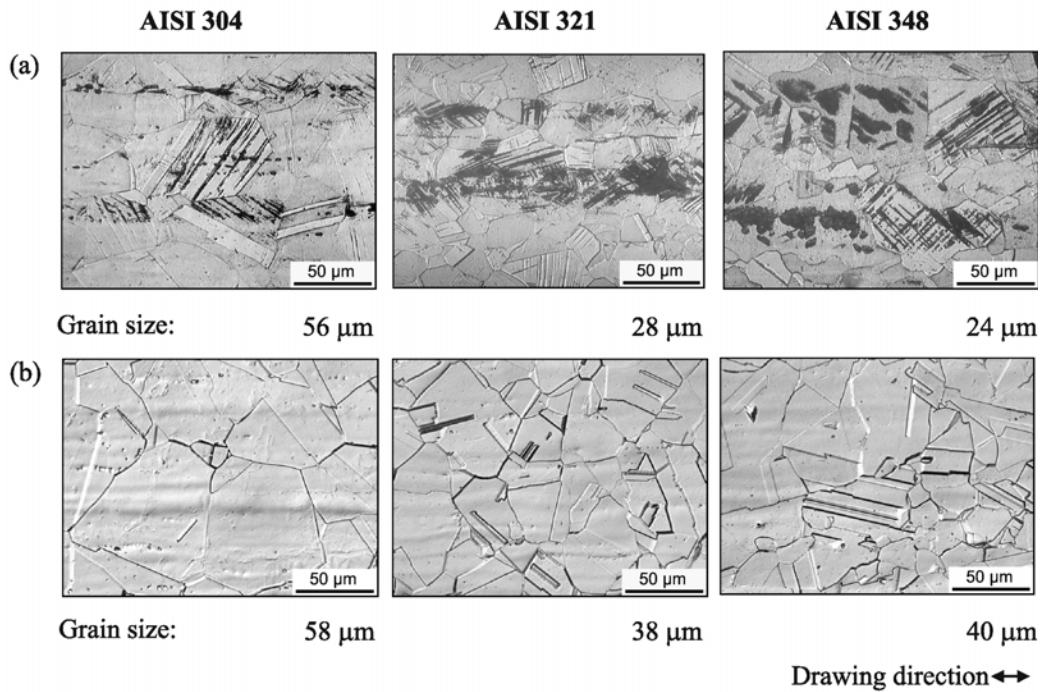


Fig. 2: Optical micrographs in the as-received condition (a) and after solution annealing (b)

To eliminate α' -martensite formed during manufacturing and to obtain a homogeneous microstructure, solution annealing at $T = 1050^\circ\text{C}$ for 35 min with subsequent quenching in water was performed. Fig. 2 shows optical micrographs in the as-received condition (a) and after solution annealing (b). Due to the heat treatment dark bands of α' -martensite caused by manufacturing (a) were transformed into austenite (b). Even after solution annealing the material is characterized by a banded structure in drawing direction e. g. due to elongated non-metallic inclusions and/or sulfides. There was no α' -martensite detected after specimen preparation.

3. Experimental methods

Axial constant amplitude tests were performed on servohydraulic testing systems under plastic strain control with a load ratio of $R_e = -1$ and a frequency of 0.2 Hz using triangular load-time functions at ambient temperature. In order to characterize the change in magnetic properties during cyclic loading additional constant amplitude tests under total strain control with $\varepsilon_{a,t} = 6.0 \cdot 10^{-3}$ at $f = 0.2$ Hz and $\varepsilon_{a,t} = 2.5 \cdot 10^{-3}$ at $f = 5$ Hz, respectively were performed. Stress-strain-hysteresis measurements and the change in specimen temperature ΔT , measured with thermocouples fixed on the specimen surface were used to describe the cyclic deformation behavior [8]. Three thermocouples T_1 - T_3 were fixed on the specimen surface for highly accurate temperature measurements. The cross-section at the attachment points of T_2 and T_3 (shafts) is much bigger compared to the one at T_1 . Thus, temperature changes $\Delta T = T_1 - 0.5 \cdot (T_2 + T_3)$ are only caused by plastic deformation in the gauge length. The plastic deformation at the test frequency 0.2 Hz and plastic strain amplitudes in the range $2 \cdot 10^{-3} \leq \varepsilon_{a,p} \leq 6 \cdot 10^{-3}$ lead to a maximum temperature increase of $\Delta T \leq 20$ K in the gauge length (cf. Fig. 5). Therefore a temperature influence on the deformation-induced α' -martensite formation can be neglected.

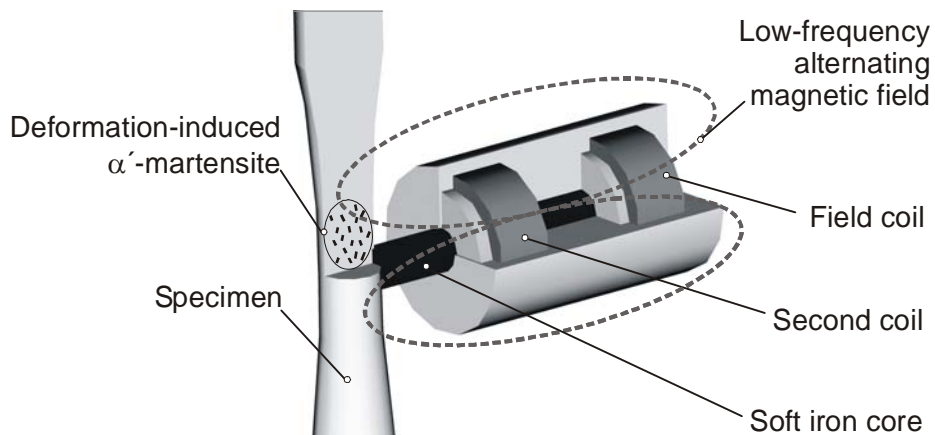


Fig. 3: Measuring principle of ferritescope

In order to quantify the phase transformation from austenite to α' -martensite and to calculate the fatigue life, the deformation-induced α' -martensite fraction ξ was measured in-situ with a ferritescope sensor, which is calibrated for the measurement of δ -ferrite. According to the magnetic induction method in the ferritescope a magnetic field generated by a coil interacts with the magnetic volume fraction of the specimen. The change in the magnetic field induces a voltage proportional to the magnetic fraction in a second coil (Fig. 3). Since the magnetic permeability of α' -martensite is a function of total strain [13], the ferritescope data F (%-ferrite) have to be converted to the actual α' -martensite fraction ξ according to the linear correlation $\xi = 1.7 \cdot F$ (%-martensite) [14]. Furthermore, the change in magnetic induction $\delta\xi$ measured by ferritescope is converted to %-martensite and divided by 100 %-martensite. Consequently, $\delta\xi$ is a non-dimensional figure.

4. Results

In Fig. 4 the load-dependent development of the stress amplitude σ_a is plotted versus the number of cycles N . The σ_a , N -curves of AISI 304 indicate for $\varepsilon_{a,p} = 2$ to $5 \cdot 10^{-3}$ initial cyclic softening followed by pronounced cyclic hardening. The cyclic deformation curves of AISI 321 and 348 illustrate in a similar way cyclic hardening processes after an initial load-dependent period with nearly constant σ_a -values. Cyclic hardening is caused by an increase of the number of stacking faults [1] and an increase of the dislocation density in the austenite [2], as well as the deformation-induced α' -martensite formation (see Fig. 6). Pronounced cyclic hardening enhances the stress amplitude at specimen failure in the range of the tensile strength (Tab. 2) of the solution-annealed austenites AISI 304, AISI 321 and AISI 348.

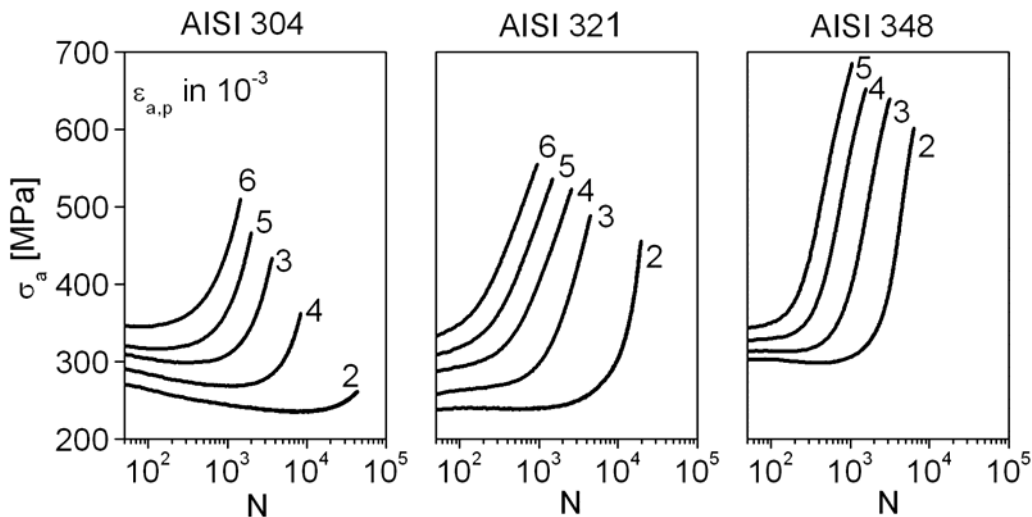


Fig. 4: Development of the stress amplitude σ_a as function of number of cycles N

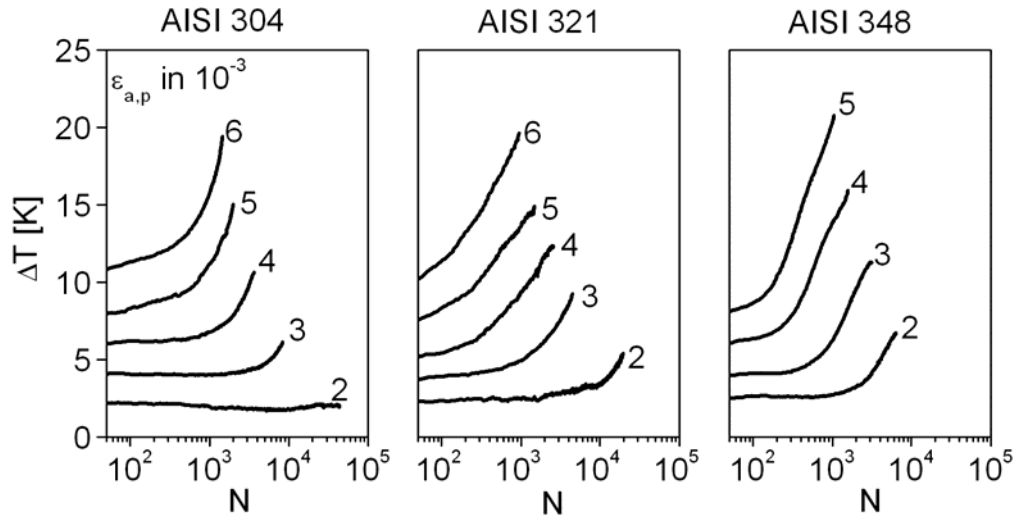


Fig. 5: Development of the change in the temperature ΔT as function of number of cycles N

In addition to Fig. 4, the cyclic deformation behavior can be described in a comparable manner by the change of the specimen temperature ΔT due to cyclic plastic deformation (Fig. 5). The $\Delta T, N$ -curves indicate maximum temperature changes $\Delta T \leq 20$ K which do not significantly influence the plasticity-induced formation of α' -martensite.

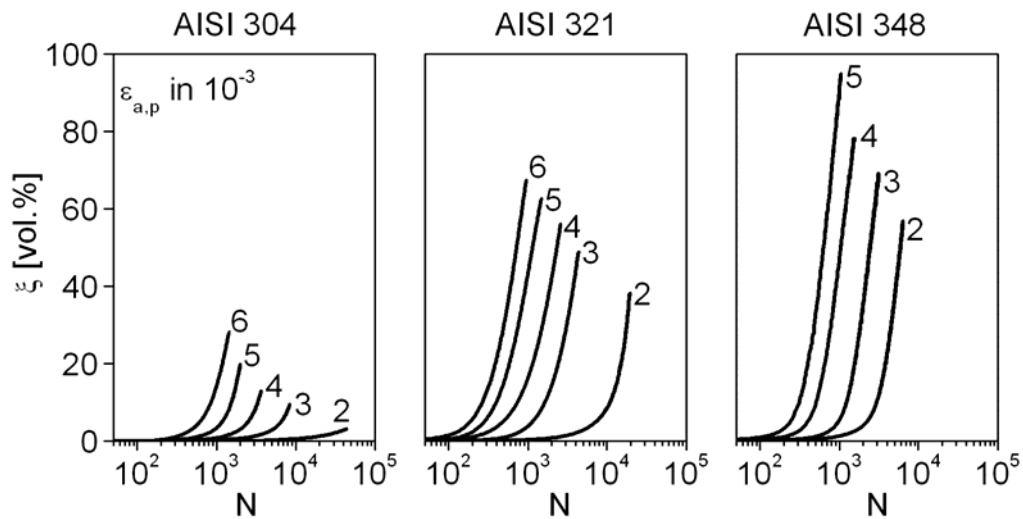


Fig. 6: Development of the α' -martensite as function of number of cycles N

The development of deformation-induced α' -martensite formation under cyclic loading is shown in Fig. 6. The α' -martensite fraction increases continuously with increasing number of cycles. With increasing plastic strain amplitude the α' -martensite fraction ξ increases earlier and reaches higher values at specimen failure.

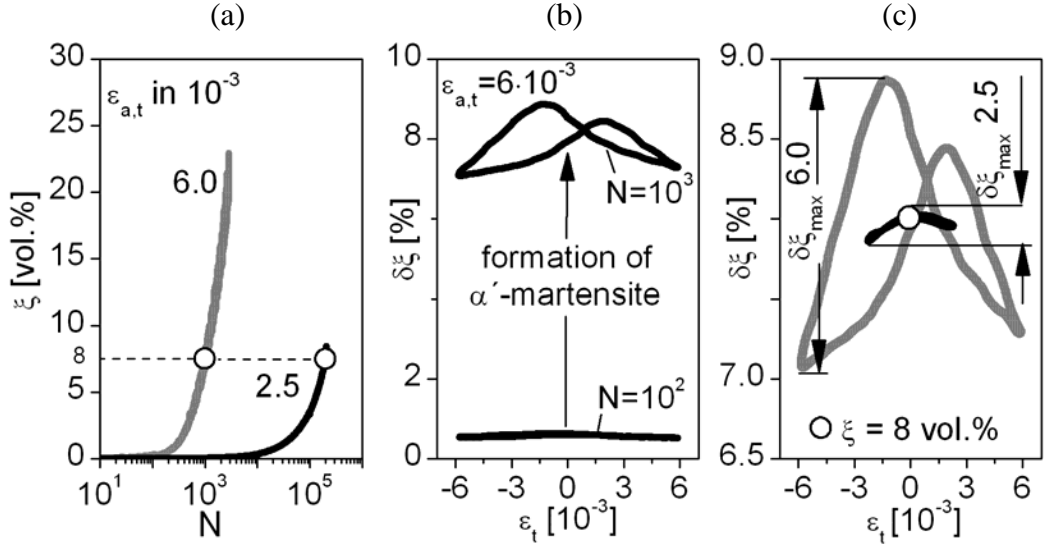


Fig. 7: Development of the α' -martensite fraction under total strain control (a), magnetic-mechanical hysteresis loops (b) as well as magnetic-mechanical hysteresis loops for a constant α' -martensite fraction (c) for AISI 321

For a detailed characterization of the change in magnetic properties under cyclic loading, constant amplitude tests under total strain control at $\varepsilon_{a,t} = 2.5 \cdot 10^{-3}$ and $\varepsilon_{a,t} = 6.0 \cdot 10^{-3}$ for AISI 321 were performed. The course of α' -martensite formation is plotted versus the number of cycles in Fig. 7. With increasing total strain amplitude the ξ values increase earlier and reach a higher maximum at specimen failure. Figure 7b shows the change in magnetic properties for $\varepsilon_{a,t} = 6.0 \cdot 10^{-3}$ within the cycles $N = 10^2$ and $N = 10^3$. Due to the Villari effect [15] and spontaneous switching of magnetic domains, characteristic magnetic-mechanical hysteresis loops in form of butterfly curves develop (cf. Fig. 7b and Fig. 7c). Under total strain control the maximum change of specimen's length is constant in the fatigue test. Therefore, the maximum change in magnetic induction within one cycle strongly depends on the α' -martensite fraction and increases with increasing α' -martensite fraction. Additionally, for the same α' -martensite fraction, e.g. $\xi = 8$ vol.%, higher total strain amplitudes cause higher maximum changes in magnetic induction (Fig. 7c).

Figure 8 describes a method for fatigue life calculation on the basis of magnetic properties in a schematic manner. As mentioned above, the deformation-induced α' -martensite fraction increases continuously with increasing plastic (Fig. 6) or total (Fig. 7a) strain amplitude and increasing number of cycles. But the information about the absolute α' -martensite fraction alone is not sufficient to define the actual fatigue state. For example, the same α' -martensite fraction can be achieved at different fatigue lives: $\xi = 8$ vol.% for $\varepsilon_{a,t} = 6.0 \cdot 10^{-3}$ at 50 % N_f and for $\varepsilon_{a,t} = 2.5 \cdot 10^{-3}$ just before failure at 95 % N_f (Fig. 7a). Hence for a reliable fatigue life calculation on the basis of magnetic measurements, besides the α' -martensite fraction the change in magnetic induction a correlation with the load

amplitude (Fig. 7c) is needed. The proposed fatigue life calculation method for metastable austenitic steels is based on the ratio between the maximum change in magnetic induction $\delta\xi_{\max}$ within one cycle and the α' -martensite fraction ξ . Both values can be measured with a high-precision magnetic ferritescope.

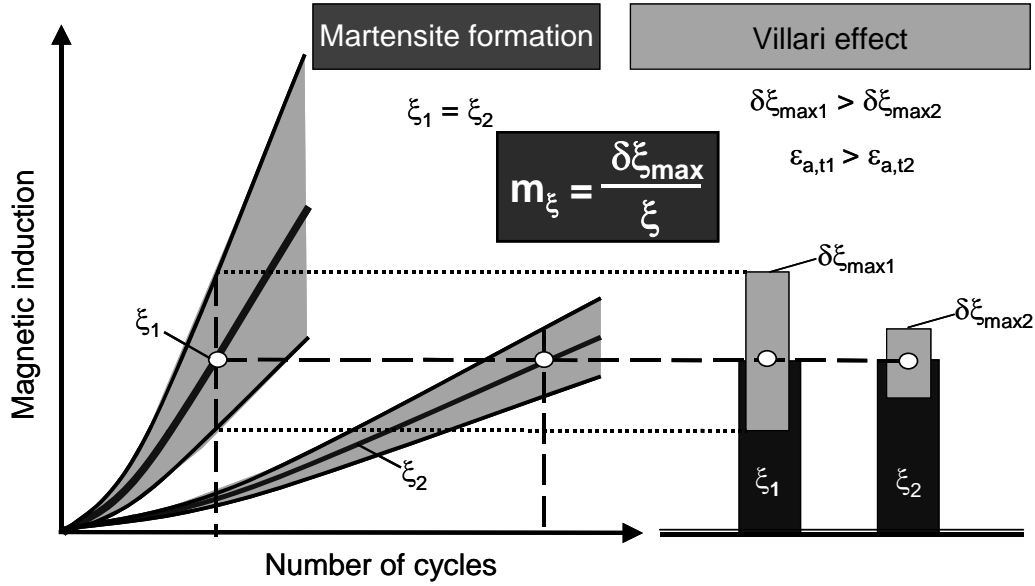


Fig. 8: Fatigue life calculation method for metastable austenitic steels on the basis of magnetic measurements

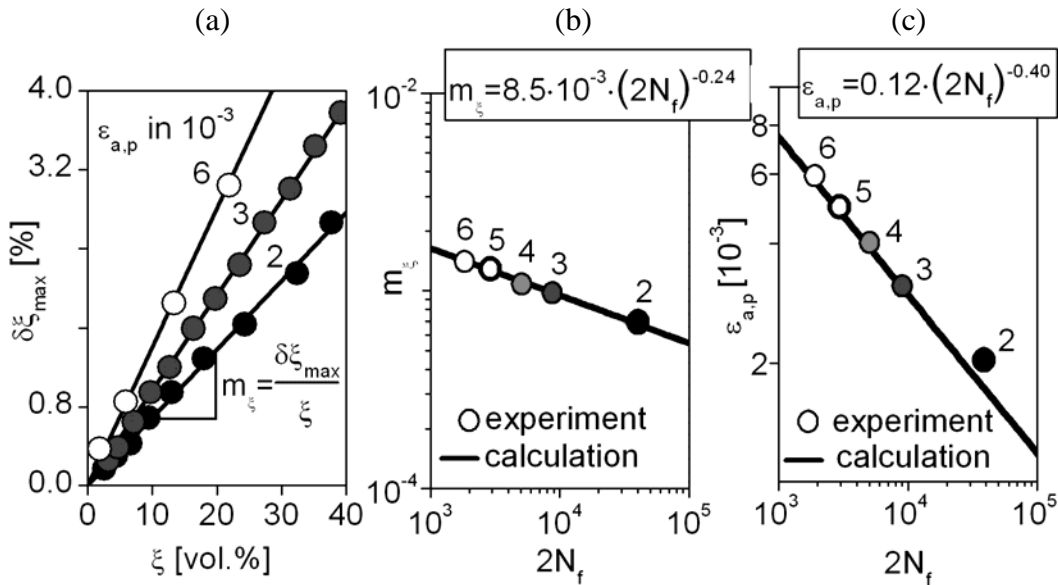


Fig. 9: Maximum change in magnetic induction versus α' -martensite fraction (a), fatigue life calculation on the basis of magnetic measurements (b) and the plastic strain amplitude (c) for AISI 321

By illustrating the change in magnetic induction $\delta\xi_{\max}$ as a function of the α' -martensite fraction ξ , a constant magnetic relation parameter m_ξ results for

each loading amplitude (Fig. 9a). The relation between m_ξ and the number of cycles to failure N_f can be calculated in excellent agreement with experimental data by the function $m_\xi = \varepsilon'_{B, \xi} (2N_f)^{c_\xi}$ (Fig. 9b), in analogy to the Coffin-Manson equation (Fig. 9c).

4. Conclusions

The metastable austenitic steels AISI 304, AISI 321 and AISI 348 are characterized by a plasticity-induced phase transformation from paramagnetic austenite to ferromagnetic α' -martensite under cyclic loading. The chemical composition has a fundamental influence on the austenite stability, which can be described with M_S for thermally induced α' -martensite formation and M_{d30} temperature for deformation-induced α' -martensite formation. Due to minimum M_S and M_{d30} temperatures AISI 304 is more stable compared to titanium-alloyed AISI 321 and niobium-alloyed AISI 348 steels. Due to pronounced cyclic hardening stress amplitudes in the range of the tensile strength of the solution-annealed austenites are reached. In addition to stress-strain hysteresis measurements, the cyclic deformation behavior can be described in a comparable manner by the change of the specimen temperature ΔT due to cyclic plastic loading. The α' -martensite formation can be measured non-destructively with a ferritescope. Due to the Villari effect and the spontaneous switching of magnetic domains, magnetic-mechanical hysteresis loops in form of butterfly curves develop. The formation of α' -martensite and the maximum change in magnetic induction were used for the determination of the fatigue state and fatigue life calculation of the investigated metastable austenitic steels. The fatigue life calculation leading to an excellent agreement with experimental data is based on the ratio between the maximum change in magnetic induction and α' -martensite fraction. The relation between the magnetic relation parameter and the number of cycles to failure can be described in analogy to the Coffin-Manson equation.

5. References

- [1] M. Bayerlein, H.-J. Christ, H. Mughrabi, Plasticity-induced martensitic transformation during cyclic deformation of AISI 304L stainless steel, *Mat. Sci. Eng. A* 114 (1989) L11-L16
- [2] H.-J. Bassler, D. Eifler, Cyclic deformation behaviour and plasticity-induced martensite formation of the austenitic steel X6CrNiTi1810, in: X.R. Wu, Z.G. Wang (Eds.), *Fatigue 99*, 1, Higher Education Press, Beijing, 1999, pp. 205-210
- [3] H. Oettel, U. Martin, The nature of TRIP-effect in metastable austenitic steels, *Int. J. Mat. Res.* 97 (2006) 1642-1647
- [4] B.A. Behrens, S. Hübner, C. Sunderkötler, J. Knigge, K. Weilandt, K. Voges-Schwiger, Local strain hardening of sheet and solid forming components during formation of martensite in metastable austenitic steels, *Adv. Mater. Res.* 22 (2007) 5-15

- [5] M. Smaga, F. Walther, D. Eifler, Deformation-induced martensitic transformation in metastable austenitic steels, *Mat. Sci. Eng. A* 483-484 (2008) 394-397
- [6] T. Angel, Formation of martensite in austenitic stainless steels, *J. Iron Steel Inst.* (1954) 165-174
- [7] G.B. Olson, M. Cohen, Kinetics of strain-induced martensitic nucleation, *Metall. Trans.* (1975) 791-795
- [8] M. Smaga, F. Walther, D. Eifler, Investigation and modelling of the plasticity-induced martensite formation in metastable austenites. *Int. J. Mat. Res.* 97 (2006) 1648-1655
- [9] U. Krupp, C.G. West, H. Duan, H.-J. Christ, Strain-induced martensite formation in metastable austenitic steels with varying carbon content, *Z. Metallkd.* 93 (2002) 706-711
- [10] J. Schreiber, U. Cikalova, Y. Vertyagina, Use of the fractal nature of spatial and temporal response behavior for materials damage characterization, in: P.D. Portella, T. Beck, M. Okazaki (Eds.), *LCF-6*, Berlin, 2008, pp. 665-660
- [11] P.E. Grayson, W. Law, L.D. Thompson, *Civil Eng. - ASCE* 68, 7 (1998) 68-71
- [12] H. Becker, H. Brandis, W. Küppers, Zur Verfestigung instabil austenitischer nichtrostender Stähle und ihre Auswirkung auf das Umformverhalten von Feinblechen, *Thyssen Edelst. Techn. Berichte* 12, Band Heft 1 (1986) 35-54
- [13] S.S. Hecker, J.L. Smith, K.P. Staudhammer, M.G. Stout, Effects of strain state and strain rate on deformation-induced transformation in 304 stainless steel: Part I. magnetic measurements and mechanical behaviour, *Metall. Trans.*, (1982) 619-626
- [14] J. Talonen, P. Aspegren, H. Hänninen, Comparison of different methods for measuring strain induced α' -martensite content in austenitic steels, *Materials Science and Technology*, 20 (2004) 1506-1512
- [15] E. Villari, Ueber der Aenderungen des magnetischen Moments, welche der Zug und das Hindurchleitung eines galvanischen Stromes in einem Stabe von Stahl oder Eisen hervorbringen, *Ann. der Phy. und Chemie*, 126, T. 87, (1865) 87-122

Acknowledgments

The support of this work by the German Research Foundation (Deutsche Forschungsgemeinschaft) is gratefully acknowledged.